YMTHE, Volume *27*

Supplemental Information

A Stem Cell-Based Screening Platform Identifies Compounds that Desensitize Motor Neurons to Endoplasmic Reticulum Stress

Sebastian Thams, Emily Rhodes Lowry, Marie-Hélène Larraufie, Krista J. Spiller, Hai Li, Damian J. Williams, Phuong Hoang, Elise Jiang, Luis A. Williams, Jackson Sandoe, Kevin Eggan, Ivo Lieberam, Kevin C. Kanning, Brent R. Stockwell, Christopher E. Henderson, and Hynek Wichterle

Supplemental materials and methods

Automated image analysis

To assess the number of "healthy" fluorescent cells exhibiting outgrowths >5 times the cell body diameter (assessment of overall survival) and to evaluate the mean neurite length per cell (assessment of neurite growth). These parameters were used consistently throughout the study.

Small molecule screen

We consistently observed that the ratio of surviving untreated G93A mutant motor neurons to untreated wild-type motor neurons was ~0.83; in order to detect compounds acting synergistically to the genotype, all data were normalized to this ratio. Compounds resulting in a G93A-to-WT survival ratio of <0.67-fold, corresponding to a 50% difference in survival, were re-tested in five-point 2-fold dilution series. All hit compounds were evaluated visually, and wells with apparent artefacts such as auto-fluorescence and excessive cell clumping were removed. Compounds that were generally toxic, i.e., that resulted in lower survival than the controls with low trophic support for both genotypes, were rescreened in 1:10 dilution series. After completion of screen data collection, images for all hit compounds were individually evaluated in blinded manner. Wells with overall low survival or artefacts (e.g. precipitation, auto-fluorescence or significant cell detachment, were excluded for further analysis). The remaining compounds were tested in 8-point dose response titrations, in FACS-purified cultures and in an independent pair of mutant-wild type cell lines.

Immunohistochemistry

Cultures were washed three times with 0.01 M PBS containing 0.3% Triton-X, prior to incubation with secondary antibodies (Alexa donkey 488/555/647) for 60 min in room temperature. The following primary antibodies were used: mouse Hb9 and mouse islet1/2 from Hybridoma Bank (1:100); mouse Human nuclear antigen from Millipore (MAB1281, clone 235-1, 1:1000); Tuj-1 from Neuromics or EMD Millipore (1:500); and phospho c-jun from Cell Signalling (1:100). Slides were examined in either a Zeiss AxioObserver with a Coolsnap HQ_2 camera (Photometrics), a Zeiss LSM Meta 510 or a Zeiss LSM 880 Axioobserver Z1 confocal microscope. Images were processed and sometimes cropped in Adobe Photoshop (Creative suit 6, Adobe Systems) for presentations purpose, changes were applied to the entire image, and in equal proportions to all images from the same.

Calcium imaging

On day three post-dissociation, coverslips were incubated with 5 μM Fura-2 AM, ratiometric calcium indicator dye (Life Sciences, USA) for 30 minutes at room temperature. After washing, coverslips were mounted on a Nikon Eclipse TE 3500 inverted microscope equipped with a 40× 1.30 NA objective (Nikon, USA), a pco.EDGE CMOS camera (pco, Germany), a Lambda LS light source, a Lambda LS-2 filterwheel with 340 nm and 380 nm excitation filters (both Sutter, USA). Images were first acquired using bright field and a fluorescent filter to identify cells to analyze at later steps. Drug applications were carried out using a custom-built focal application system located approximately 100 μm from the field of view. A 5 s baseline for the Fura-2 signal was then acquired, followed by a 1 s pulse of 100 μM kainic acid (KA). Epifluorescent images were captured at a rate of 1 image/sec for 1 min, switching between 340 and 380 nm filters every 500 ms. Cells were allowed to recover for 2 min, and only coverslips where cells returned to baseline were analyzed further. The coverslips were then continuously exposed to 7.5 μM CPA while 1 image/30 sec was acquired for 20 min, followed by a 2 min recovery, and finally a second pulse of KA. Following acquisition, the 340/380 ratio of each pair of images was calculated on a pixel by pixel basis using FIJI software v. 1.4 (www.fiji.sc). Regions of interest were drawn manually using the morphology of the cells from a single 340 image as a template. Quantification was carried out using Igor Pro v. 6 (Wavemetrics, USA). The rate at which the evoked calcium transients returned to the baseline was calculated from the tau (time constant) of a single exponential curve fitted to the falling part of the Ca intensity trace from 80% to 20% of the peak. Only neurons that recovered to 10% of the peak ratio value were included in the analysis.

qPCR primers

Xbp1_1_fwd	ACA CGC TTG GGA ATG GAC AC
Xbp1_1_rev	CCA TGG GAA GAT GTT CTG GG
Xbp1_2_fwd	GAA TGC CCA AAA GGA TAT CAG ACT C
Xbp1_2_rev	GGC CTT GTG GTT GAG AAC CAG GAG
p58ipk_fwd	TGG ACT TTA CTG CCG CAA GA
p58ipk_rev	CGT CAA GCT TCC CTT GTT TGA
Gapdh_fwd	CAT GGC CTT CCG TGT TCC TA
Gapdh_rev	GCG GCA CGT CAG ATC CA
Erdj4_fwd	CCT TTC ACA AAT TAG CCA TGA AGT AC
Erdj4_rev	TGC TTC AGC ATC AGG GCT TT
Chop_fwd	AGG AGC CAG GGC CAA CA
Chop_rev	TCT GGA GAG CGA GGG CTT T
Cd59a_fwd	GCT GCT TCT GGC TGT GTT CTG
Cd59a_rev	GTT GGA AAC AGT GGT AGC ATG TG
Bloc1s1_fwd	CAG GCC TAC ATG AAC CAG AGA AA
Bloc1s1_rev	GGC AGC CTG GAC CTG TAG AG
Nfkb2_fwd	GTG GGC AAG CAG TGT TCA GA
Nfkb2_rev	TCA TGT CCT TGG GTC CTA CAG A
Tnfrsf10b_fwd	CGT CTC ATG CGG CAG TTG
Tnfrsf10b_rev	TCG GCT TTG ACC ATT TGG A
Creb3l3_fwd	CCA GCT GCC TCT CAC CAA GT
Creb3l3_rev	CCG GAT CTT TCT GCG GAT T
Noxa_fwd	CTG TGG TTC TGG CGC AGA T
Noxa_rev	GGG CTT GGG CTC CTC ATC
Nrf2_fwd	TTC CCG TGA GTC CTG GTC AT
Nrf2_rev	AGC GGC TTG AAT GTT TGT CTT T
Tap1_fwd	TTG GCC CGA GCC TTG A
Tap1_rev	TGG TGG CAT CAT CCA AGA TAA G
Bip_fwd	AGC CAT CCC GTG GCA TAA
Bip_rev	GGA CAG CGG CAC CAT AGG
Calr_fwd	GCC AGA CAC TGG TGG TAC AGT TC
Calr_rev	CGC CCC CAC AGT CGA TAT T
Gadd45a_fwd	GAC GAC GAC CGG GAT GTG
Gadd45a_rev	AGC AGA ACG CAC GGA TGA G
Atf4_fwd	CGA TGC TCT GTT TCG AAT GGA
Atf4_rev	CCA ACG TGG TCA AGA GCT CAT

RNA-sequencing

RNA was isolated in duplicates from FACS-purified untreated, CPA treated and CPA + TUDCA treated MNS of both genotypes ($hSOD1^{WT}$ and $hSOD1^{G93A}$), as described for RT-qPCR reactions. Poly-A pull-down was then used to enrich mRNAs from total RNA samples (1 µg per sample, RIN >8) and libraries were prepared using Illumina TruSeq RNA prep kit (San Diego, CA). Libraries were then sequenced using an Illumina HiSeq 2000 instrument (Columbia Genome Center, Columbia University). Read alignment and gene levels were calculated using Cufflinks and Tophat softwares. Raw FastQ sequencing data and processed normalized expression data (RPKM) were compared between. All genes associated with ER stress and associated pathways, suggested in the current literature, were selected for further analysis.

Generation isogenic human embryonic stem cell lines by genetic targeting

After corroborating the desired SOD1 gene edit (Fig. S5B-C), we directed the differentiation of SOD +/A4V and SOD1+/+ HUES3 Hb9::GFP cells into cultures containing spinal motor neurons. GFP^{+} motor neurons of both genotypes could be isolated using FACS (Fig. S5F), and SOD1 transcript and protein expression in these cells was confirmed (Fig. S5D-E). The new lines were further validated by staining for motor neuron transcription factor Islet1 (Fig. S5G) and assessment of survival in short and long term cultures (Figure S5H and J).

In vivo administration of TUDCA

Drug was administered every three days from P30 to P51 for a total of 7 injections. At P51, mice were deeply anesthetized using ketamine/xylazine and intracardially perfused with ~15 mL room temperature phosphate-buffered saline (PBS) followed by ~30 mL of 4% PFA. Following dissection, tibialis anterior (TA) muscles were washed in PBS overnight, and then processed for cryoprotective embedding. To visualize NMJs, 30 μm longitudinal cryosections of the whole TAs were incubated with α-bungarotoxin conjugated to Alexa Fluor 488 (1:500; Invitrogen) and an antibody to vesicular acetylcholine transporter (VAChT; raised in rabbit, Covance 1:32,000) to label motor endplates and nerve terminals, respectively. Because a lack of co-localization indicated muscle denervation, % NMJ innervation was determined by dividing the total number of areas of overlap between VAChT and BTX signals (total number innervated endplates) by the number of areas containing BTX signal (total number of endplates). One TA was assessed for each animal (n=4-6), with every third section throughout the whole muscle stained and counted such that a minimum of 1000 NMJs were evaluated per animal. Images were acquired using a Nikon Eclipse TE-2000-E fluorescence microscope with a 4x or 10x objective. All animal work was performed in compliance with Columbia University IACUC protocols.

Statistics

For cell cultures, a minimum of three independent experiments were generally performed, which was considered sufficient based on previous experience with this type of assays where culture conditions and cell lines were kept constant. For *in vivo* experiments, a power analysis based on pilot studies was performed to estimate the number of animals required to detect the studied effects. Data sets are expressed as mean value +/- SEM throughout the paper. Statistical analyses were performed with Graph Pad Prism (v. 7, GraphPad Software Inc.) or R' (www.r-project.org). If normal distribution and equal variance could be assumed, analysis of significance was performed with an unpaired two-tailed Student's t-test for pairwise comparison, or a One-way Anova with *post hoc* Dunnet's multiple comparison test. Otherwise, analysis was instead performed by Mann-Whitney Rank sum test or Kruskal-Wallis test with Dunn's multiple comparison *post hoc* test. Statistical significance is indicated by * $P<0.05$, ** $P<0.01$, *** $P<0.001$. Unless stated otherwise, each *N* represents an independent experiment or animal. In the few events where only one biological replicate was analyzed, the technical replicates were used to generate histograms, as stated in the figure legends when applicable. Statistical analyses were not performed on any of these data.

Figure S1

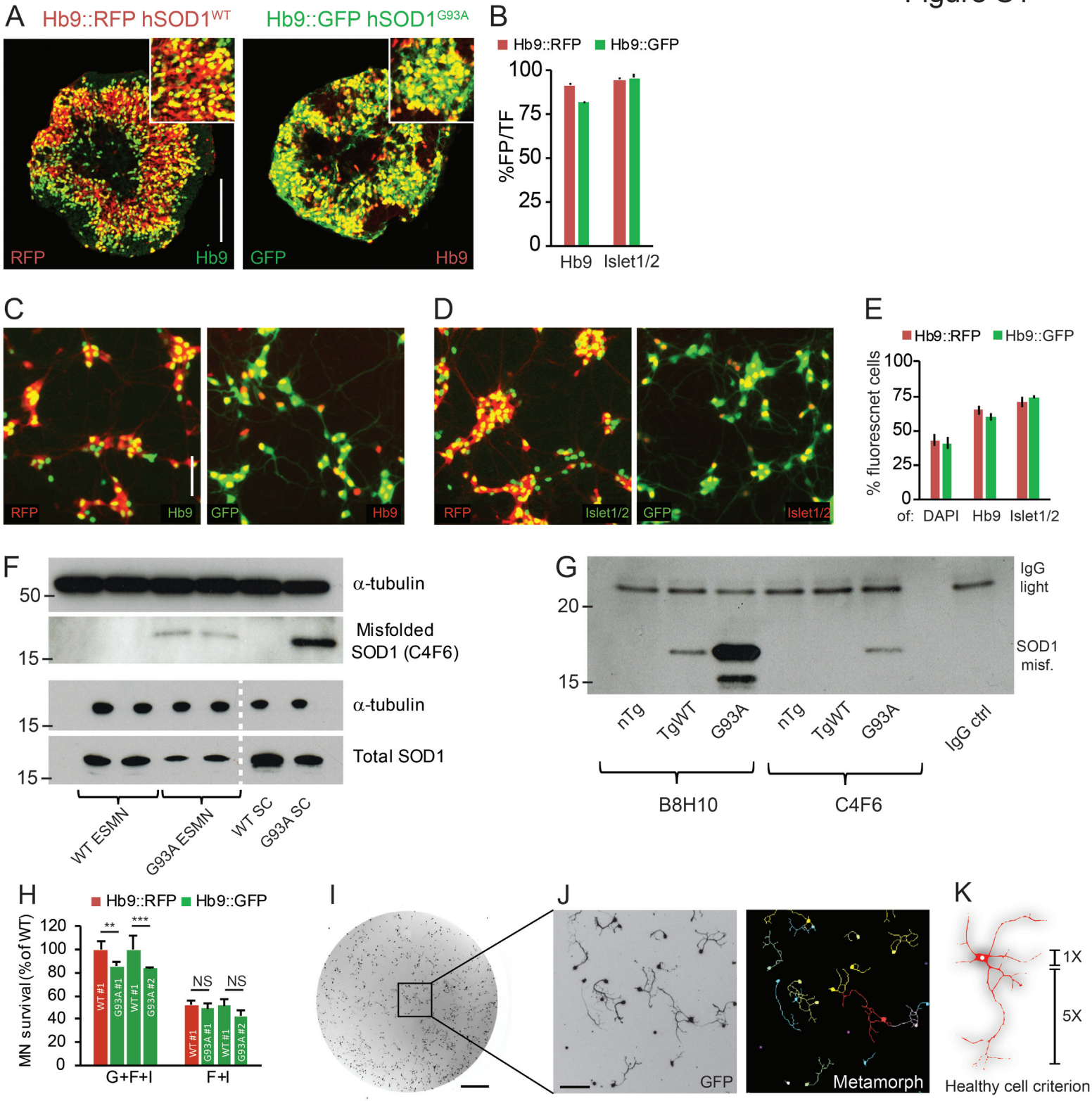
A
Hb9::RFP hSOD1WT
Hb9::GFP hSOD1G93A
RFP
Hb9
GFP
Hb9
B
Hb9::RFP
Hb9::GFP
%FP/TF
100
75
50
25
0
Hb9
Islet1/2
C
RFP
Hb9
GFP
Hb9
D
RFP
Islet1/2
GFP
Islet1/2
E
Hb9::RFP
Hb9::GFP
% fluorescnet cells
100
75
50
25
0
of:
DAPI
Hb9
Islet1/2
F
50
15
15
15
α-tubulin
Misfolded SOD1 (C4F6)
α-tubulin
Total SOD1
WT ESMN
G93A ESMN
WT SC
G93A SC
G
20
15
IgG light
SOD1 misf.
nTg
TgWT
G93A
nTg
TgWT
G93A
IgG ctrl
B8H10
C4F6
H
Hb9::RFP
Hb9::GFP
MN survival (% of WT)
120
100
80
60
40
20
0
**
***
NS
NS
WT #1
G93A #1
WT #1
G93A #2
WT #1
G93A #1
WT #1
G93A #2
G+F+I
F+I
I
J
GFP
Metamorph
K
1X
5X
Healthy cell criterion

Fig S2

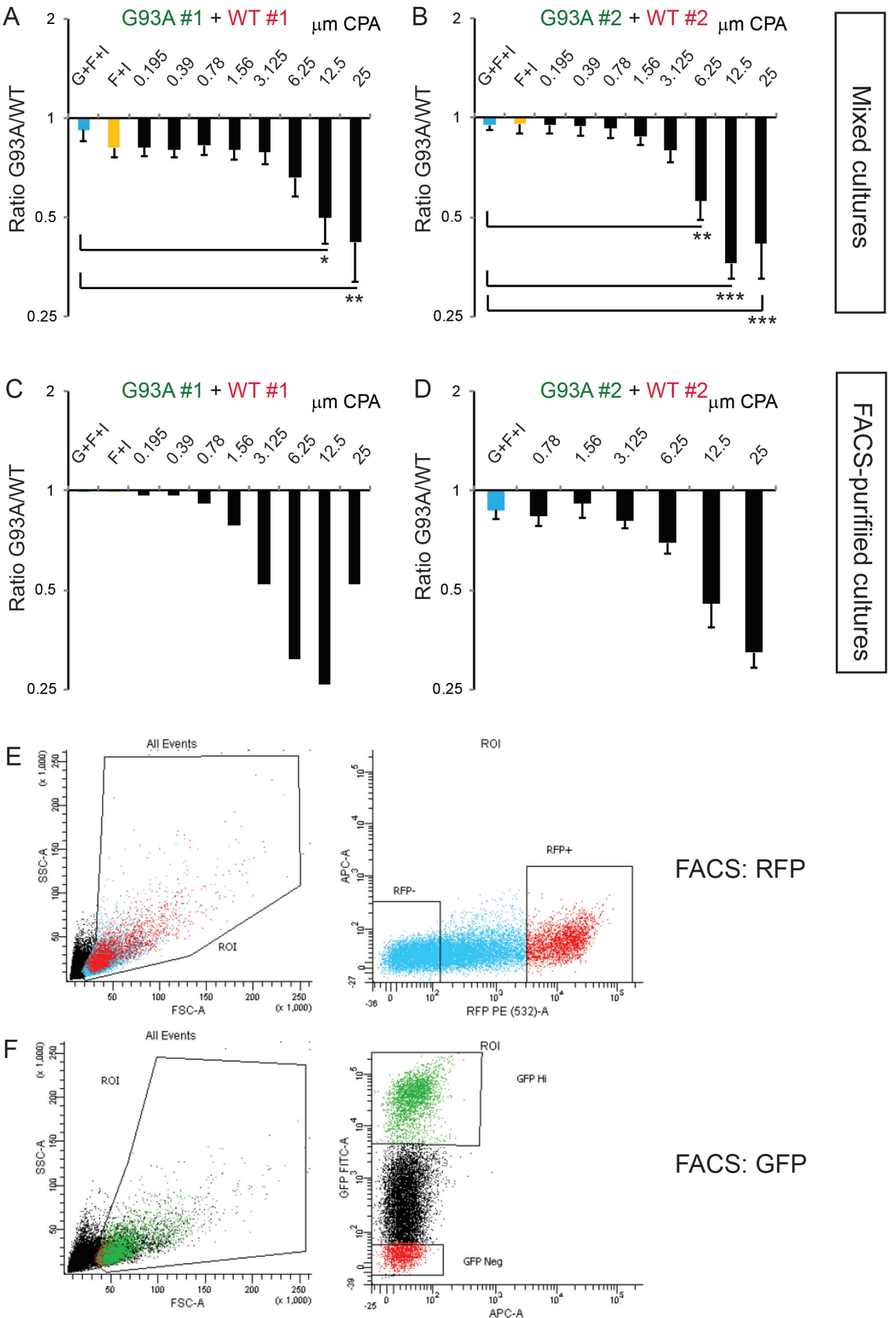
A
G93A #1 + WT #1
µm CPA
Ratio G93A/WT
G+F+I
F+I
0.195
0.39
0.78
1.56
3.125
6.25
12.5
25
B
G93A #2 + WT #2
Mixed cultures
C
G93A #1 + WT #1
D
G93A #2 + WT #2
FACS-purifiied cultures
E
All Events
SSC-A
FSC-A
ROI
RFP-
RFP+
APC-A
RFP PE (532)-A
FACS: RFP
F
GFP Hi
GFP Neg
GFP FITC-A
APC-A
FACS: GFP

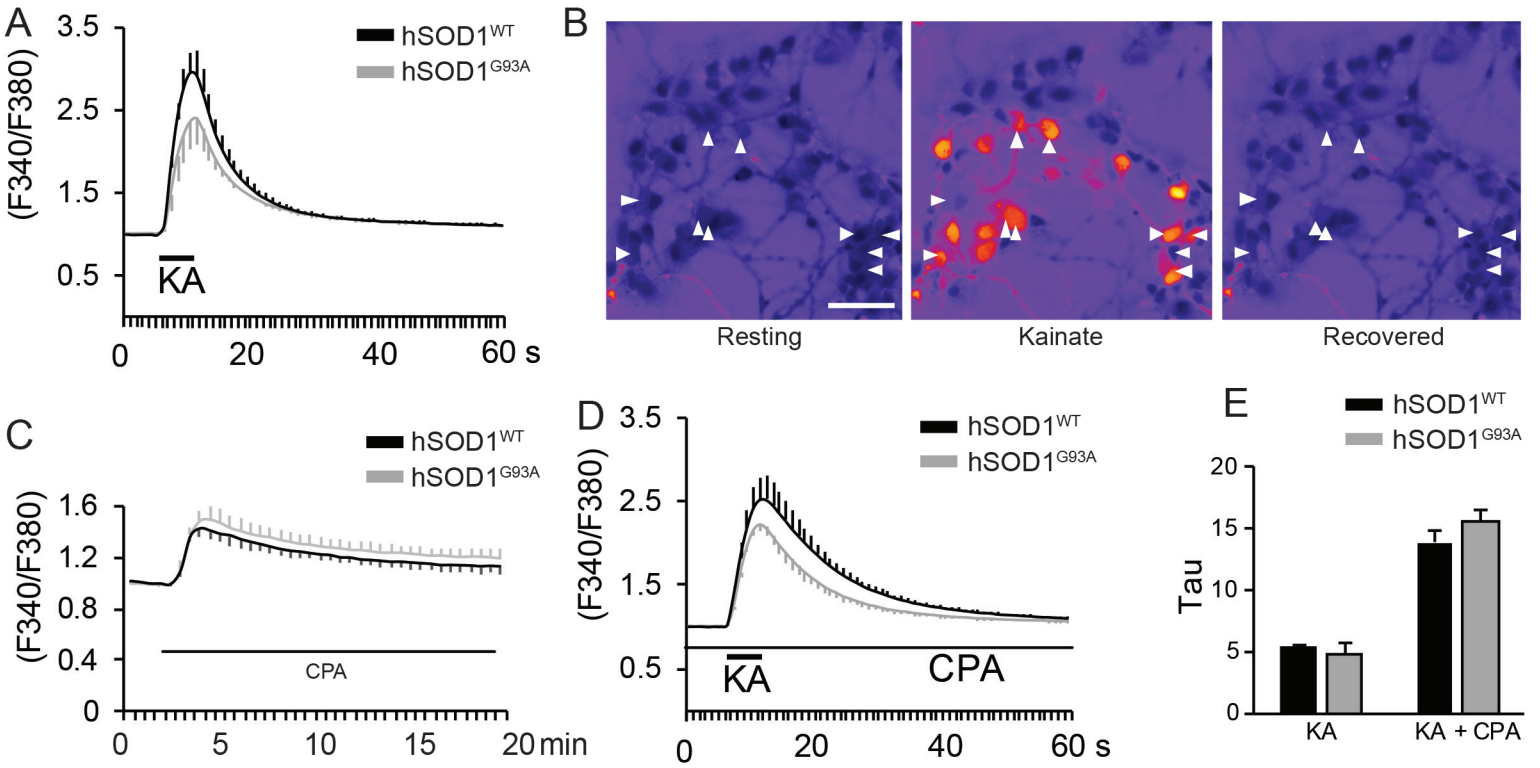
A
3.5
2.5
1.5
0.5
(F340/F380)
hSOD1WT
hSOD1G93A
KA
0
20
40
60 s
B
Resting
Kainate
Recovered
C
hSOD1WT
hSOD1G93A
1.6
1.2
0.8
0.4
0
(F340/F380)
CPA
0
5
10
15
20 min
D
3.5
2.5
1.5
0.5
(F340/F380)
hSOD1WT
hSOD1G93A
KA
CPA
0
20
40
60 s
E
hSOD1WT
hSOD1G93A
20
15
10
5
0
Tau
KA
KA + CPA

Fig. S4

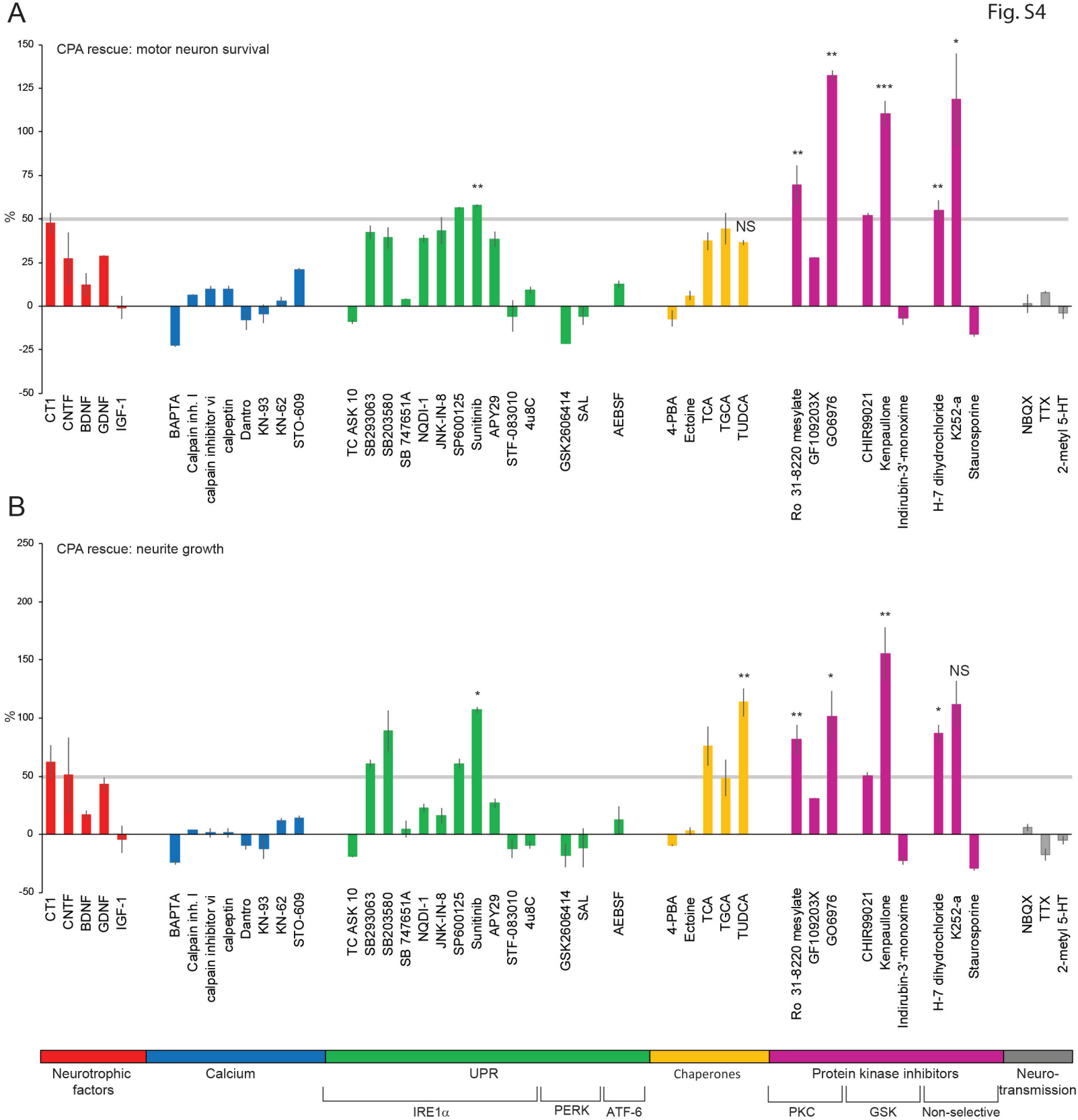
A
CPA rescue: motor neuron survival
%
CT1
CNTF
BDNF
GDNF
IGF-1
BAPTA
Calpain inh. I
calpain inhibitor vi
calpeptin
Dantro
KN-93
KN-62
STO-609
TC ASK 10
SB293063
SB203580
SB 747651A
NQDI-1
JNK-IN-8
SP600125
Sunitinib
APY29
STF-083010
4u8C
GSK2606414
SAL
AEBSF
4-PBA
Ectoine
TCA
TGCA
TUDCA
Ro 31-8220 mesylate
GF109203X
GO6976
CHIR99021
Kenpaullone
Indirubin-3'-monoxime
H-7 dihydrochloride
K252-a
Staurosporine
NBQX
TTX
2-metyl 5-HT
NS
B
CPA rescue: neurite growth
Neurotrophic factors
Calcium
UPR
IRE1α
PERK
ATF-6
Chaperones
Protein kinase inhibitors
PKC
GSK
Non-selective
Neuro-transmission
C
MN survival (%of CTRL)
CTRL
TUDCA
TDCA
TLCA
TCA
UDCA
TCDCA
GUDCA
TGCA
GCDCA
GCA
TMCA
CPA
D
Neurite growth (%of CTRL)

Figure S5

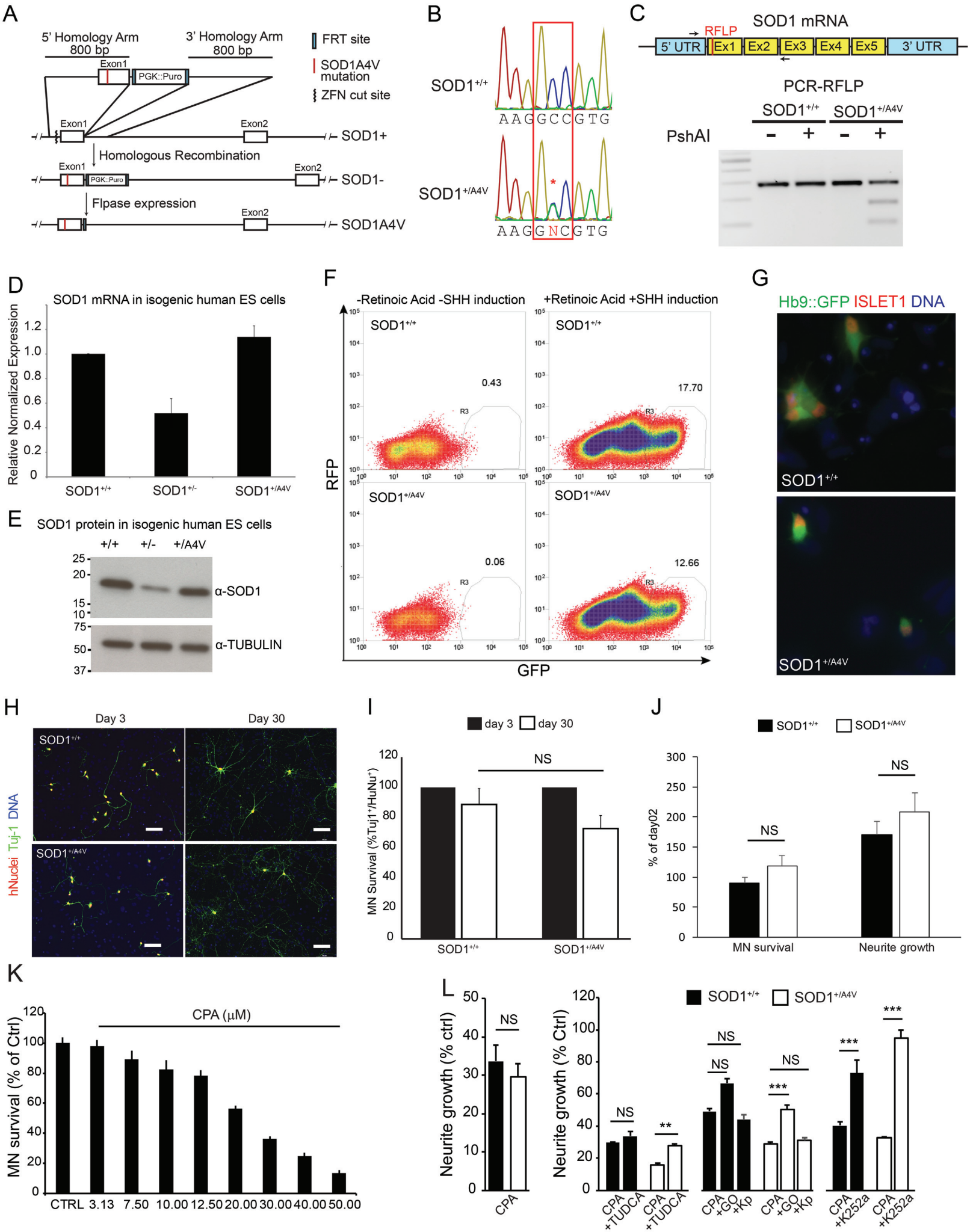
A
5' Homology Arm 800 bp
3' Homology Arm 800 bp
FRT site
SOD1A4V mutation
ZFN cut site
Exon1
PGK::Puro
Exon2
SOD1+
Homologous Recombination
SOD1-
Flpase expression
SOD1A4V
B
SOD1+/+
AAGGCCGTG
SOD1+/A4V
AAGGNCGTG
C
SOD1 mRNA
RFLP
5' UTR
Ex1
Ex2
Ex3
Ex4
Ex5
3' UTR
PCR-RFLP
SOD1+/+
SOD1+/A4V
PshAI
D
SOD1 mRNA in isogenic human ES cells
Relative Normalized Expression
SOD1+/+
SOD1+/-
SOD1+/A4V
E
SOD1 protein in isogenic human ES cells
+/+
+/-
+/A4V
α-SOD1
α-TUBULIN
F
-Retinoic Acid -SHH induction
+Retinoic Acid +SHH induction
RFP
GFP
0.43
17.70
0.06
12.66
R3
G
Hb9::GFP ISLET1 DNA
H
Day 3
Day 30
hNuclei Tuj-1 DNA
I
day 3
day 30
MN Survival (%Tuj1+/HuNu+)
NS
J
% of day02
MN survival
Neurite growth
K
CPA (μM)
MN survival (% of Ctrl)
CTRL 3.13 7.50 10.00 12.50 20.00 30.00 40.00 50.00
L
Neurite growth (% ctrl)
Neurite growth (% Ctrl)
CPA
CPA +TUDCA
CPA +GO +Kp
CPA +K252a

Fig. S6

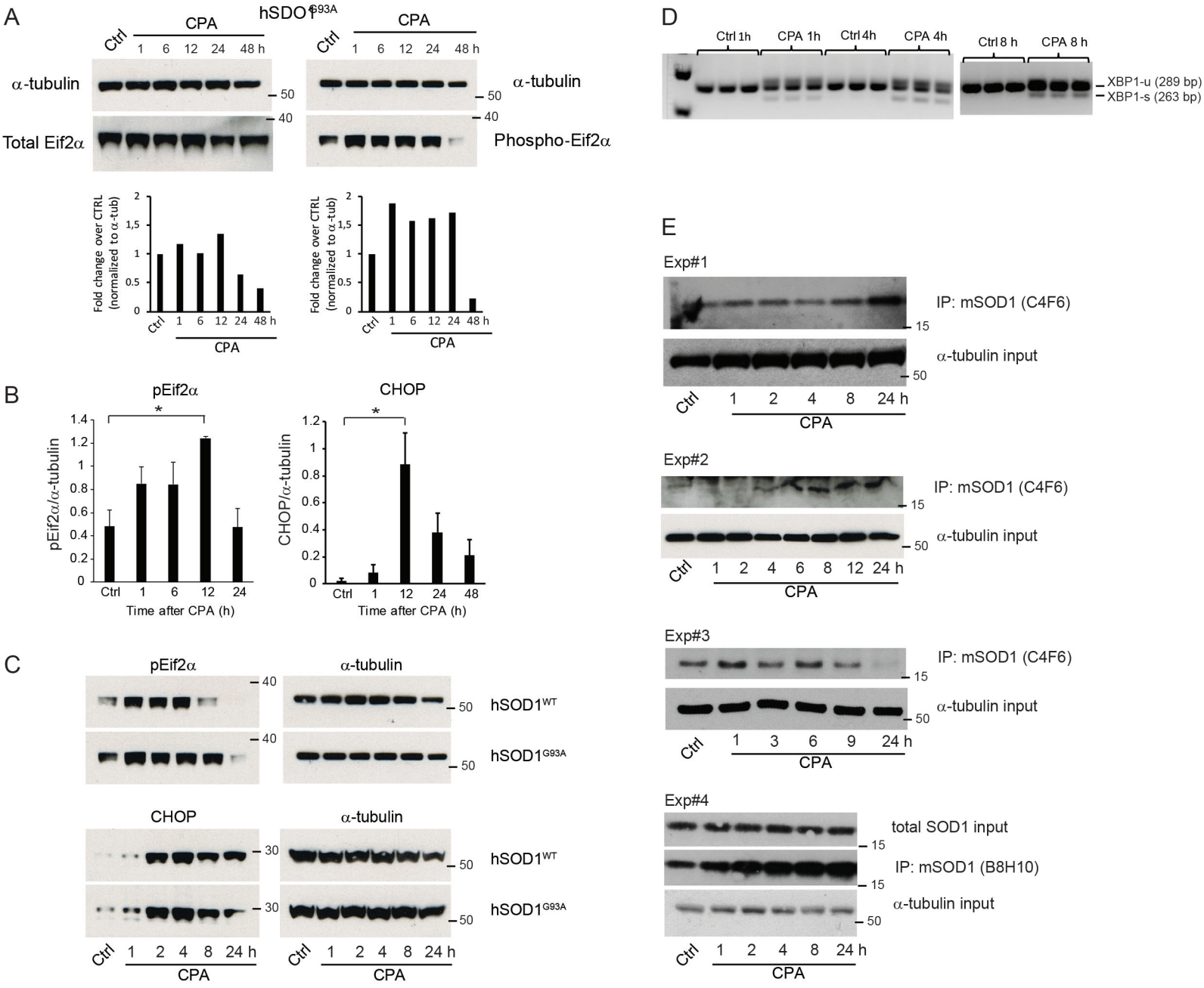
A
hSDO1G93A
CPA
Ctrl
1 6 12 24 48 h
α-tubulin
Total Eif2α
Phospho-Eif2α
50
40
Fold change over CTRL (normalized to α-tub)
B
pEif2α
CHOP
pEif2α/α-tubulin
CHOP/α-tubulin
Time after CPA (h)
C
hSOD1WT
hSOD1G93A
Ctrl 1 2 4 8 24 h
D
Ctrl 1h
CPA 1h
Ctrl 4h
CPA 4h
Ctrl 8 h
CPA 8 h
XBP1-u (289 bp)
XBP1-s (263 bp)
E
Exp#1
Exp#2
Exp#3
Exp#4
IP: mSOD1 (C4F6)
α-tubulin input
total SOD1 input
IP: mSOD1 (B8H10)

Fig. S7

A

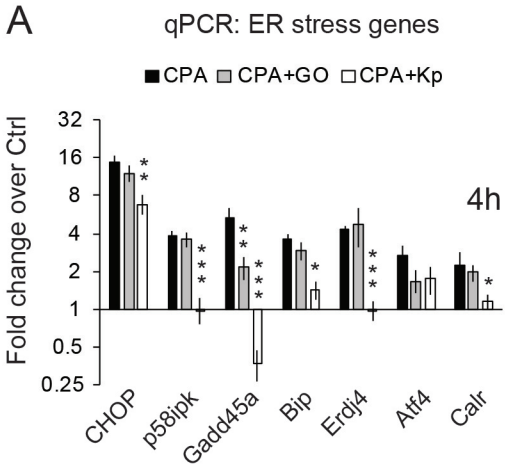

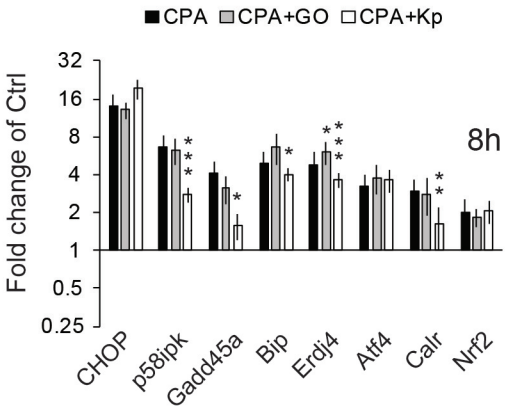

C

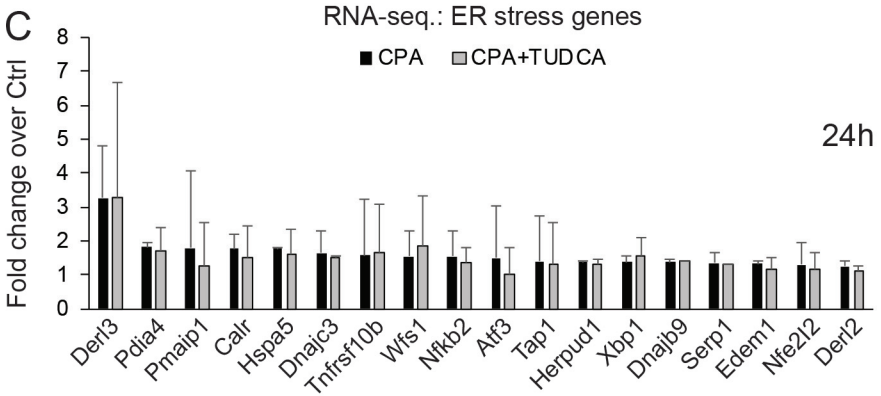

B

Genes	Pathway
CHOP	Induced by ER stress, mediates apoptosis.
p58ipk	Exerts negative feed back loop on PERK pathway
GADD45a	Activates p38/JNK, regulated by-AP1 and ATF-4.
Bip	UPR initiating factor.
Erdj4	ER protein, induced by ER stress, regulates activity of 70kDa heat shock proteins.
Atf4	UPR/PERK pathway.
Calr	Ca^{2}-dependent ER chaperone.
Nrf2	UPR/PERK pathway. Survival promoting transcription factor.

Figure legends

Figure S1. Evaluation of newly derived transgenic ES lines, biochemical analysis of normal- and misfolded SOD1 expression in differentiated cells, and survival motor neuron derived from cell-lines expressing different fluorescent reporters. **(A)** Confocal micrographs showing sections of embryoid bodies from Hb9::RFP hSOD1^{WT} and Hb9::GFP hSOD1^{G93A} stained for motor neuron transcription factors Hb9 and Islet1/2. Scale bar 100 μm. **(B)** Measurements of the overlap between fluorescent reporter protein (FP) and transcriptions factors (TF). Bars denote averages, error bars indicate SEM. **(C-E)** Light microscopy micrographs (**C-D**) and histogram (**E**) showing reporter validation in differentiated new ES lines (two lines for each reporter were differentiated in two separate rounds, results are presented as mean value/reporter). Scale 50 μm. Bars denote means and error bars SEM. **(F)** Cropped images of immunoblots showing expression of total and misfolded (C4F6) SOD1 in untreated motor neuron cultures. P100 spinal cords from WT or SOD1^{G93A} mice were used as controls. The dashed line indicates were the lower image was cropped. **(G)** Immunoblot showing the specificity for the C4F6 andf B8H10 antibodies for misfolded mutant SOD1. **(H)** Motor neuron survival in transgenic hSOD1 WT and G93A cell lines expressing different fluorescent reporters. Survival was assessed in medium (G+F+I) and low (F+I) neurotrophic support in either mixed red-green cultures (red WT #1 + green G93A #1, n=6) or separate cultures (green WT #1, green G93A #2, n=3). Bars denote average, error bars indicate SEM, **p<0.01 ***p<0.001 (Unpaired two-tailed Student's t-test). **(I)** Representative whole-well image of live cells, acquired with the Trophos Plate Runner^{HD}. Scale bar 1 mm. **(J)** Magnification of **(I)** and the result of automated image analysis using Metamorph software. Scale bar 50 μm. **(K)** 'Healthy cell criterion' using presence of a significant neurite to distinguish live cells from fluorescent debris.

Figure S2. Evaluation of CPA toxicity in two independent pair of cell lines, in mixed and FACS-sorted motor neuron cultures. (A-D) Dose response curves for motor neuron survival after CPA treatment in two independent pairs of WT-G93A cell lines (compiled results are shown in Fig. 1D and E). Cultures were either unpurified (**A-B**) or purified using FACS (**C-D**) (**A:** n=5, **B:** n=4, **C:** n=6 culture wells, **D:** n=2). Bars denote average, error bars indicate SEM, *p<0.05, **p<0.01, ***p<0.001 (One-way Anova, *post hoc* Dunnet's multiple comparison test). **(E-F)** Scatter plots showing representative gates for FACS-purification of reporter lines.

Figure S3. Calcium homeostasis in Hb9::RFP hSOD1^{WT} and hSOD1^{G93A} motor neurons exposed to kainic acid and CPA. Biochemical analysis of normal- and misfolded SOD1 expression in differentiated cells. (A) Kainic acid (KA)-induced change in cytoplasmic Ca^{++} was assessed by calculating 340/380 nm ratio in Fura-2 labelled purified hSOD1^{WT} and hSOD1^{G93A} MN cultures. **(B)** Representative example still images of KA-induced calcium transients. Scale bar 50 μm. Images are pseudocolored using the Lookup table 'fire' function in FIJI (increase in calcium is shown in warm colors). The slope of decrease in Fura-2 ratio (Tau) was measured in cultures exposed to kainic acid (KA) in absence or presence of CPA. **(C)** CPA-induced change in cytoplasmic Ca^{++} was assessed by calculating 340/380 nm ratio in Fura-2 labelled purified hSOD1^{WT} and hSOD1^{G93A} MN cultures. **(D)** Kainic acid (KA)-induced change in cytoplasmic Ca^{++} in the presence of CPA was assessed by calculating 340/380 nm ratio in Fura-2 labelled purified hSOD1^{WT} and hSOD1^{G93A} MN cultures (n=5 for WT, n=4 for G93A, for all analyzes). Bars denote average, error bars indicate SEM. **(E)** The slope of decrease in Fura-2 ratio (Tau) was measured in cultures exposed to kainic acid (KA) in absence or presence of CPA.

Figure S4. Selected results from the ER stress rescue screen and mini screen for bile acid derivatives. **(A-B)** Effects of rescue compounds on survival and neurite growth in CPA treated motor neuron cultures. Compounds are subcategorized and color-coded based on their putative mechanisms of action. Bars denote average, error bars indicate SEM (n=3-6 culture wells/compound). The cut-off level for further analysis is indicated by a grey line. Top compounds were compared to CPA only (n=3-6), *p<0.05, **p<0.01, ***p<0.001 (unpaired two-tailed Student's t-test or a Mann-Whitney Rank sum test). **(C-D)** Mini screen for survival (**C**) and neurite rescue (**D**) effects of bile acid derivatives. Each compound was screen in three different concentrations with 5X dilution steps. Bars denote average, error bars indicate SEM (n=3).

Figure S5. Generation of human isogenic cell lines to study aspects of ALS pathogenesis *in vitro*.

(A) Diagram of gene targeting strategy for introduction of the SOD1A4V mutant allele into the SOD1 locus of HUES3 Hb9::GFP. **(B)** Sequencing of the SOD1 locus. **(C)** PCR-RFLP analysis for a unique PshAI restriction site confirmed correct targeting. **(D-E)** qRT-PCR (**D**) and immunoblot (**E**) assays for SOD1 expression in targeted stem cell lines demonstrated reduced levels of the SOD1 transcript and protein levels. **(F)** FACS plots depicting a distinct population of differentiated cells which express the GFP reporter. Differentiated neural cells

not exposed to the MN patterning molecules RA and SAG were used as negative control to gate for green fluorescence. **(G)** Hb9::GFP^{+} cells express the transcription factor Islet1 confirming spinal MN identity. **(H-I)** Cell survival assays in mixed cultures indicate a trend for reduced survival in isogenic human ESC MNs expressing the SOD1^{A4V} variant relative to the isogenic control (**I**). Representative images (**H**) of Human Nuclei and Tuj1 staining at days 3 and 30 (P = 0.09, n= 4). Scale bar 100 μm **(J)** Short term assessment (5 days post dissociation) of MN survival and neurite growth in FACS-purified human isogenic lines, assessed by calcein labelling in live cultures. **(K)** Histogram showing a dose response survival curve for CPA toxicity in purified human SOD1$^{+/A4V}$ ESC MNs. Bars denote average, error bars indicate SEM (n=3 culture wells/concentration). **(L)** Histogram showing neurite growth in purified isogenic human motor neuron cultures. Cells were grown under control conditions, treated with CPA or pretreated with rescue compounds followed by CPA (n=9 for CPA vs. CTRL for both genotypes, (n=3 for rescue compounds for both genotypes). Bars denote average, error bars indicate SEM, *p<0.05, **p<0.01, ***p<0.001 (the effect of CPA was compared between WT vs. ALS MNs, as indicated with a line; the effects of rescue compounds were compared to CPA for each genotype).

Figure S6. Biochemical analysis of UPR mediators and misfolded SOD1.

(A) Western blot showing protein levels of total (left) and phosphorylated Eif2α (right) in cultures treated with CPA. α-tubulin served as loading control. Eif2α bands were quantified and normalized to the loading control, as displayed in the histograms. **(B)** Histograms showing quantification of replicate blots for pEif2α (n=3-7) and CHOP (n= 2-6), and their loading controls (α-tubulin). Bars denote means +/- SEM, *p<0.05 (One-way Anova, *post hoc* Dunnet's multiple comparison test for pEif2α and a Kruskal-Wallis test with Dunn's multiple comparison *post hoc* test for CHOP). **(C)** Western blot showing induction of two UPR markers, pEif2α and CHOP, in hSOD1^{WT} and hSOD1^{G93A} motor neuron cultures. α-tubulin was used as loading control. Please note that hSOD1^{G93A} blot for pEif2α is the same as presented in panel (A). **(D)** Gel image used for quantification of spliced/unspliced XBP1. **(E)** Biological replicate blots for IP lysate and input two antibodies (C4F6 and B8H10) to analyze misfolded SOD1 levels, α-tubulin was used as loading control. Experiment #4 shows that the levels of total SOD1 is unchanged after exposure to CPA.

Figure S7. Analysis of ER stress-associated genes in cultures treated with CPA and rescue compounds.

(A) Histograms showing qPCR results for the ER stress panel for genes that were ≥2-fold upregulated by CPA and ≥2-fold downregulated in hSOD1^{G93A} motor neuron cultures at 4 and/or 8 hours by at least one of the two tested compounds (GO=GÖ6967, Kp=kenpaullone). RNA was extracted from unpurified hSOD1^{G93A} motor neurons (n=3, independent culture dishes). Bars denote average, error bars indicate SEM. CPA was compared to CPA+rescue compounds for each gene and time point, *p<0.05, **p<0.01, ***p<0.001 (One-way Anova, *post hoc* Dunnet's multiple comparison test; or Kruskal-Wallis test with Dunn's multiple comparison *post hoc* test). **(B)** Table showing pathways for the genes displayed in (A). **(C)** Selected results from an RNA-sequence analysis in purified hSOD1^{G93A} motor neurons cultures at 24 hours after exposure to CPA. The histograms shows all ER stress-associated genes that were at least 1.5-fold upregulated by CPA. Bars denote means +/- standard deviation (n=2).

Supplemental table 1

CPA RESCUE SCREEN	% rescue of CPA toxicity	% rescue of CPA toxicity	
Compound	**Cell death**	**Neurite growth**	**Category/pathway**
DCA	20.50911675	33.79013629	Bile acids
CA	17.11925797	67.46744235	Bile acids
HDCA	10.18137182	22.25725601	Bile acids
CDCA	11.22034401	18.22205814	Bile acids
LCA	9.085736241	22.6248862	Bile acids
nor-DCA	14.57261804	19.56389175	Bile acids
HDCA-Me ester	7.110779149	18.92722876	Bile acids
6-Et-CDCA	9.986162197	38.17796374	Bile acids
dehydro-CA	12.31894361	53.84822279	Bile acids
LCA-3-sulfate disodium salt	-2.074362332	6.127374543	Bile acids
ApoCA	1.202390831	-4.777710499	Bile acids
TDCA	10.95840141	65.83163372	Taruine conjugated bile acids and analogues
TLCA	18.97294284	64.49009632	Taruine conjugated bile acids and analogues
TCA	38.08527479	93.68497917	Taruine conjugated bile acids and analogues
UDCA	18.2051565	47.99114566	Taruine conjugated bile acids and analogues
TCDCA	14.28737331	40.5870975	Taruine conjugated bile acids and analogues
GUDCA	9.970678759	41.87969468	Taruine conjugated bile acids and analogues
TGCA	44.55414037	62.09291442	Taruine conjugated bile acids and analogues
GCDCA	2.568580788	4.418783172	Taruine conjugated bile acids and analogues
GCA	23.53008464	35.87867043	Taruine conjugated bile acids and analogues
TMCA	16.10051109	31.5368093	Taruine conjugated bile acids and analogues
Ectoine	5.031032977	4.253494542	Chemical chaperons
Butylated hydroxyanisole	1.354844525	-0.941491828	Chemical chaperons
Ferrostatin-1	2.79356048	-2.344252599	Chemical chaperons
AL8810	1.258232698	-2.05527542	Chemical chaperons
PBA	-41.56239575	-11.70826719	Chemical chaperons
AK1	-23.86319535	-30.83271417	PDI inhibitors
AK2	1.337184819	-3.257907284	PDI inhibitors
AK3	-13.69763943	-15.12140467	PDI inhibitors
AK4	-39.65076275	-46.47310177	PDI inhibitors
AK5	-23.68718212	2.312235213	PDI inhibitors
AK6	3.063364798	2.312235213	PDI inhibitors
AK7	-7.303783075	-11.93026762	PDI inhibitors
AK8	-27.88593481	-36.62835997	PDI inhibitors
AK9	-0.382896758	-2.05527542	PDI inhibitors
AK10	0.714780145	-10.31330492	PDI inhibitors
AK11	1.17828197	-3.620404836	PDI inhibitors
AK12	-11.97948204	-17.65611204	PDI inhibitors
AK13	9.871088291	16.26285303	PDI inhibitors
AK14	0.788806148	1.478837654	PDI inhibitors
AK15	2.542958577	2.436655716	PDI inhibitors
H89	-30.09836713	-22.30613359	PKA inhibtor
Ro 32-0432	69.45362016	81.40427339	PKC pathway
Go 6976	132.071419	164.4046336	PKC pathway

Phorbol-12-Myristate-13-Acetate (PMA)	27.1651683	27.55476829	PKC pathway
SRI22782	-10.20702158	18.68101413	PKC pathway
H-7 dihydrochloride	65.1027217	86.7200762	PKC pathway
Staurosporine	20.47359662	14.17999838	PKC pathway
GF109203X	27.85088299	30.94050956	PKC pathway
Ro 31-8220 mesylate	69.45362016	81.40427339	PKC pathway
Calpain inh. I	6.32809798	3.560770737	Calcium signalling
calpain inh. vi	9.877545437	3.897137092	Calcium signalling
calpeptin	3.098288729	0.67757198	Calcium signalling
Dorsomorphin dihydrochloride	6.73967196	27.84365219	Calcium signalling
KN-93	-4.231510218	-9.039734584	Calcium signalling
KN-62	3.130314662	-4.057607419	Calcium signalling
SC 79	-12.66320348	24.67689953	Calcium signalling
ML-7	-16.018605	-14.00783075	Calcium signalling
BAPTA-am	-22.4076638	-23.85843413	Calcium signalling
Dantro	-7.951848422	-9.099424947	Calcium signalling
STO-609	20.72023166	14.10316415	Calcium signalling
SB203580	42.38514236	60.62167911	P38 pathway
SB293063	39.23672175	88.75752601	P38 pathway
SB747651A	19.57562965	7.742367164	P38 pathway
TC ASK 10	-1.618735713	-2.830851895	UPR: IRE1a pathway
NQDI-1	38.83991819	14.22598976	UPR: IRE1a pathway
JNK-IN-8	43.27201114	16.24361567	UPR: IRE1a pathway
SP600125	56.27881783	60.92493308	UPR: IRE1a pathway
APY29	57.75930514	106.9694934	UPR: IRE1a pathway
4u8C	9.303566151	-0.004912081	UPR: IRE1a pathway
STF-083010	9.975897399	3.15447713	UPR: IRE1a pathway
GSK2606414	21.91490255	0.731015109	UPR: PERK pathway
SAL	-5.720293345	-11.87407306	UPR: PERK pathway
AEBSF	12.53726409	12.53726409	UPR: ATF-6 pathway
K-252a	118.4447322	112.0067487	MLK pathway
Indirubin-3'-monoxime	1.508853123	-0.051027126	GSK3/CDK5 pathway
Roscovitine	5.759798441	50.80843357	GSK3/CDK5 pathway
Kenpaullone	110.5319404	155.2520568	GSK3/CDK5 pathway
CHIR99021	51.87279329	50.56491705	GSK3/CDK5 pathway
PD184352	-24.33699154	-16.25729121	MEK/ERK pathway
BRD7386	-0.290118349	-4.395083851	MEK/ERK pathway
TTX	19.50429801	0.62468452	Neurotransmission
2-metyl 5-hydroxy tryptamine	0.767196361	3.779436554	Neurotransmission
Guanabenz acetate salt	-5.953047358	-1.698662404	Neurotransmission
NBQX	1.544616023	5.665939173	Neurotransmission
DOPA	2.064118232	38.55848623	Neurotransmission
PMA	-5.730983276	25.50379088	Neurotransmission
Gambogic amide	2.750107789	39.31132329	Neurotransmission
CT1	47.45118857	62.31697159	Neurotrophic factors
CNTF	27.2134856	50.77820319	Neurotrophic factors
BDNF	12.36232474	16.59337082	Neurotrophic factors
GDNF	28.46762539	43.13787768	Neurotrophic factors
IGF-1	4.009108083	0.416651788	Neurotrophic factors
TRIM	13.72176778	53.0837837	NO signaling
CD253 (TRAIL) Antibody	-1.02268982	28.50003468	TNF superfamily & apoptosis
Caspase-8 inhibitor II	2.170111685	45.44852287	TNF superfamily & apoptosis
Sorafenib	-8.33727539	-5.065283411	Tyrosine kinase inhibitors
Sunitinib	57.75930514	106.9694934	Tyrosine kinase inhibitors
Ehop-016	-58.41396916	-44.41603223	Rac pathway
ZCL 278	3.473221912	13.44168678	Rac pathway
Fasudil	8.602455737	18.08080674	Rho pathway

PF-4708671	-11.45136888	-16.50140601	RSK inhibitor
SL0101	28.18089475	88.93617474	RSK inhibitor
PD407 5	25.41529778	NA	Chk1 pathway
NSC632839	3.12881176	10.71355041	Isopeptidase inh.
Phenazine methosulfate	-43.39544535	-18.42018807	Miscellaneous
Phenethyl isothiocyanate	-29.4794646	-5.868143127	Miscellaneous

Table S1. A screen for rescue of CPA toxicity

A list of compounds tested for their ability to reverse CPA-induced MN toxicity and/or neurite retraction. Compounds are subdivided based on putative pathways or mechanisms of action. Rescue effects are expressed as % reversal of the CPA-effect for survival and neurite growth. for the best time point (24 or 48 hrs post CPA) and concentration tested. Values either represent the averages of replicate culture wells. or from independent experiments for compounds evaluated in follow-up experiments.